

# Rapid Enzyme-Mediated Biotinylation for Cell Surface Proteome Profiling

Yanan Li, Yan Wang, Yating Yao, Jiawen Lyu, Qinglong Qiao, Jiawei Mao, Zhaochao Xu, and Mingliang Ye\*



Cite This: *Anal. Chem.* 2021, 93, 4542–4551



Read Online

ACCESS |



Metrics & More

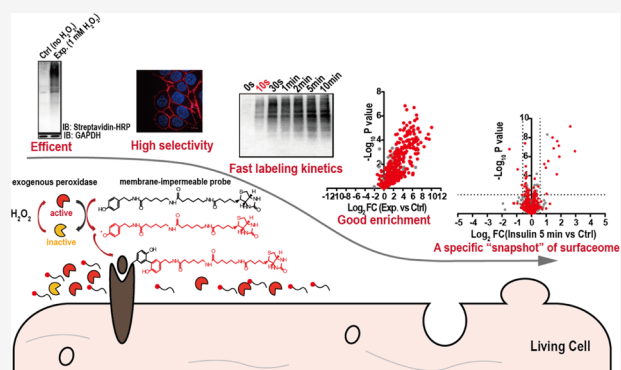


Article Recommendations



Supporting Information

**ABSTRACT:** Cell surface is the primary site for sensing extracellular stimuli. The knowledge of the transient changes on the surfaceome upon a perturbation is very important as the initial changed proteins could be driving molecules for some phenotype. In this study, we report a fast cell surface labeling strategy based on peroxidase-mediated oxidative tyrosine coupling strategy, enabling efficient and selective cell surface labeling within seconds. With a labeling time of 1 min, 2684 proteins, including 1370 (51%) cell surface-annotated proteins (cell surface/plasma membrane/extracellular), 732 transmembrane proteins, and 81 cluster of differentiation antigens, were identified from HeLa cells. By comparison with the negative control experiment using quantitative proteomics, 500 (68%) out of the 731 significantly enriched proteins ( $p$ -value < 0.05,  $\geq 2$ -fold) in positive experimental samples were cell surface-annotated proteins. Finally, this technology was applied to track the dynamic changes of the surfaceome upon insulin stimulation at two time points (5 min and 2 h) in HepG2 cells. Thirty-two proteins, including INSR, CTNBN1, TFRC, IGF2R, and SORT1, were found to be significantly regulated ( $p$ -value < 0.01,  $\geq 1.5$ -fold) after insulin exposure by different mechanisms. We envision that this technique could be a powerful tool to analyze the transient changes of the surfaceome with a good time resolution and to delineate the temporal and spatial regulation of cellular signaling.



## INTRODUCTION

A cell communicates with its environment extensively through the proteins exposed on the cell surface, termed as the cell surface proteome or surfaceome. Over the past 40 years, with the development of mass spectrometry (MS), many chemical labeling-based methods have been developed for the profiling of cell surface proteins on a proteome-wide scale.<sup>1</sup> Biotinylation of cell surface proteins on living cells by primary amine-reactive reagents, for example, sulfo-NHS-SS-biotin, is a popular method for the analysis of the surfaceome.<sup>2,3</sup> Another popular method is pioneered by Wollscheid et al., termed as cell surface capturing (CSC) technology. In the experiment, the glycans exposed on living cells are oxidized and biotinylated with biocytin hydrazide, which results in the identification of cell surface glycoproteins with very high specificity ( $\sim 90\%$ ).<sup>4,5</sup> The above methods have been successfully applied to investigate the dynamic changes of the surfaceome during cellular differentiation<sup>6,7</sup>/disease development<sup>8</sup> or in response to a stimulus.<sup>9–11</sup> However, one- or multistep long-time handling procedures (over 10 min)<sup>2,4,12–14</sup> are required for efficient labeling by these chemical-labeling strategies partly due to their slow labeling kinetics. The above studies mainly addressed the dynamic

changes of the surfaceome for a long period of time, typically for hours or even days. It can be imagined that early transient changes in the cell surface proteomes could be very important. For instance, the initial proteins that appeared on the tumor cell surface immediately upon drug treatment are more likely to drive the cell to acquire drug resistance. Unfortunately, efficient labeling methods enabling the capturing of the “snapshot” of the transient changes of surfaceome have not been reported in mammalian cells yet.<sup>6–11,15,16</sup>

In the past decade, enzyme-mediated tagging of proteins has been increasingly employed as a powerful tool for proteomic analysis. Among them, horseradish peroxidase (HRP)-mediated labeling is of particularly interest because of its rapid labeling kinetics. Generally, HRP-linked antibodies<sup>17–20</sup> or expression of HRP fusion proteins<sup>21,22</sup> are utilized to convert aryl azide-biotin reagents or phenol-biotin reagents to active

Received: November 26, 2020

Accepted: February 22, 2021

Published: March 4, 2021



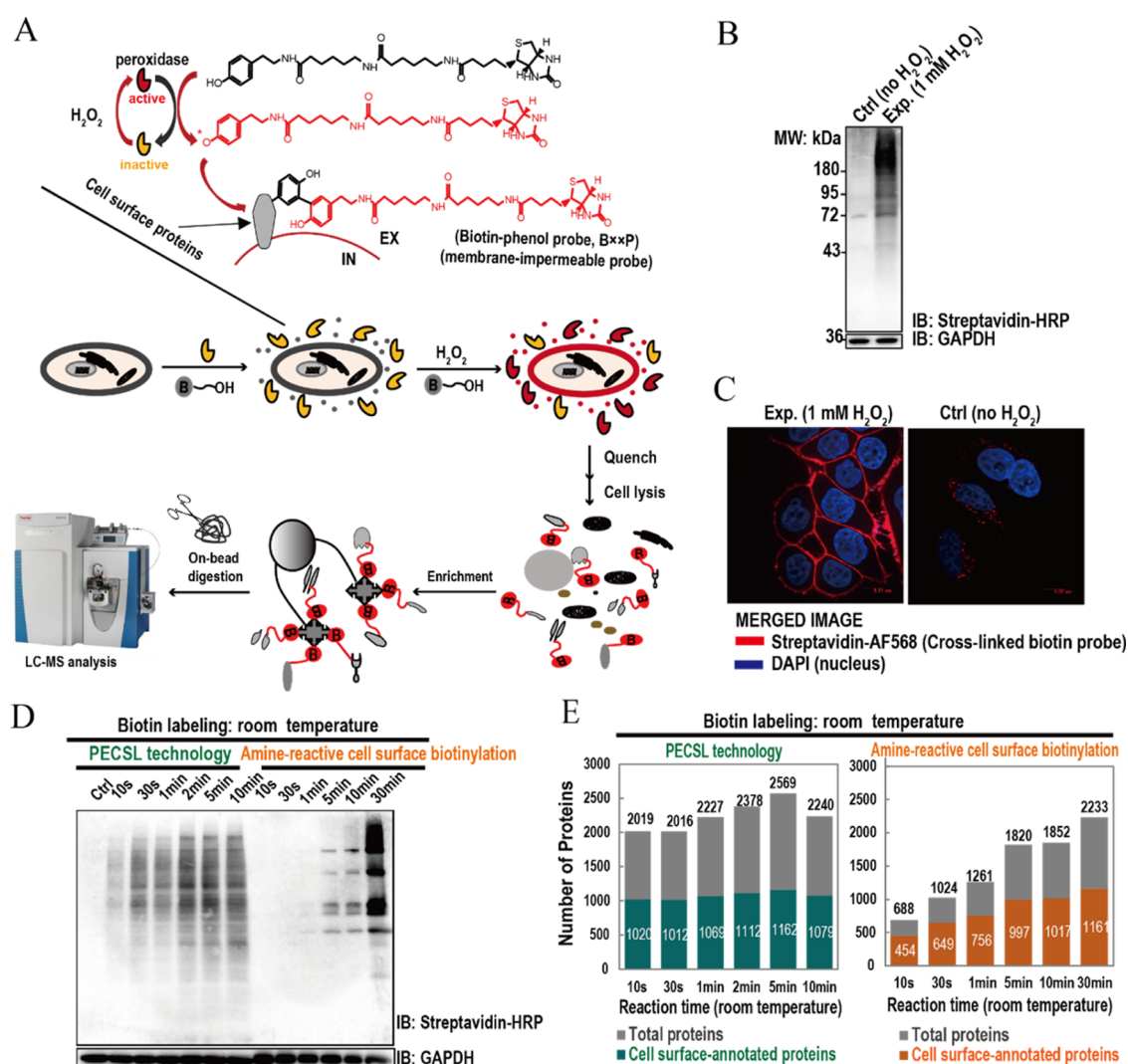


**Figure 1.** PECSL labeling enables the efficient and selective cell surface protein labeling within seconds. (A) Design of PECSL technology for surfaceome profiling. Living HeLa cells were biotinylated by 1 min-PECSL labeling and analyzed by (B) streptavidin-blot and (C) immunofluorescence assay. The time for efficient biotin labeling at room temperature was carefully evaluated for PECSL technology and amine-reactive cell surface biotinylation method using (D) streptavidin-blot and (E) single-run LC-MS/MS measurement in HeLa cells.

radical species for rapidly labeling neighboring proteins. Inspired by this, exogenous HRP and a membrane-impermeable probe are utilized in this study for the global profiling of the cell surface proteome, termed as peroxidase-mediated cell surface labeling (PECSL) strategy (Figure 1A). This novel cell surface labeling strategy enables efficient and selective cell surface labeling within seconds. One thousand three hundred and seventy cell surface-annotated proteins were identified by PECSL technology with a labeling time of 1 min in HeLa cells. By integrating with the label-free quantification (LFQ) method, we applied this fast cell surface labeling strategy to monitor dynamic changes of the surfaceome upon insulin exposure at two time points (5 min and 2 h) in HepG2 cells. Many insulin-regulated proteins were revealed, giving insight into the delineation of temporal and spatial regulation of insulin signaling.

## REAGENTS AND MATERIALS

The details are listed in the Supporting Information.

## METHODS

**Cell Culture.** Cells were cultured in RPMI 1640 medium supplemented with 10% fetal bovine serum, 1% penicillin, and streptomycin in a humidified atmosphere of 5% CO<sub>2</sub> in air at 37 °C. For each experiment, a 10 cm dish of adherent cells (~4 × 10<sup>6</sup> cells) were used.

**Insulin Treatment.** HepG2 cells at about 70% confluency were first incubated in serum free-media at 37 °C and 5% CO<sub>2</sub> overnight (16–24 h). Next, the serum-starved cells were further treated with 37 °C prewarmed media containing 200 nM insulin for 5 min or 2 h at 37 °C. In the meantime, cell samples treated with the same volume of 37 °C prewarmed insulin-free media were also prepared as controls to assess the changes in biotinylated proteins upon insulin exposure. Immediately, the media was removed, followed by two washes with room-temperature phosphate-buffered saline (PBS) and PECSL labeling for 1 min at room temperature or two washes with ice-cold PBS and amine-reactive labeling for 30 min at 4 °C.

**PECSL Labeling and Cell Lysis.** Cells at about 80% confluency were subjected to medium removal and two washes

with room-temperature PBS (0.01 M phosphate, 0.15 M sodium chloride, pH 7.4), followed by the addition of room-temperature PBS containing 0.5 mg/mL HRP (0.25 mg/mL HRP final) and 200  $\mu$ M BxxP (biotin-C6-C6-tyramine, biotin-xx-phenol probe).<sup>21</sup> Immediately, an equal volume of room-temperature PBS containing 2 mM H<sub>2</sub>O<sub>2</sub> (1 mM H<sub>2</sub>O<sub>2</sub> final) and 200  $\mu$ M BxxP was added to start labeling. The labeling reaction was gently agitated on an orbital shaker for 1 min at room temperature and then quenched using ice-cold quenching buffer (PBS, 10 mM sodium azide, 10 mM sodium ascorbate, and 5 mM Trolox). To evaluate the labeling time, PECSL labeling was performed for predetermined time points (10 s, 30 s, 1 min, 2 min, 5 min, and 10 min) at room temperature in HeLa cells. In the meantime, PBS and labeling buffers were room-temperature prewarmed.

Finally, the labeled cells were lysed with strong RIPA lysis buffer (50 mM Tris-HCl [pH 8.0], 150 mM NaCl, 0.2% sodium dodecyl sulfate, 0.5% sodium deoxycholate, 1% Triton X-100) containing 0.2% (v/v) protease inhibitor cocktail, 10 mM sodium azide, 10 mM sodium ascorbate, and 5 mM Trolox. The labeled cells were harvested by scraping on ice and lysed by sonication with 10  $\times$  30 s pulse (high, Bioruptor plus sonication device) and centrifuged at 16,000g for 15 min at 4 °C. The protein concentration of the clarified supernatant was determined by the Pierce 660 nm protein assay.

**Affinity Purification and Digestion On-Bead.** Briefly, neutravidin agarose was washed three times with PBS by centrifugation at 500g for 1 min and then incubated with the cell lysate at room temperature for 1–3 h with end-over-end mixing. After centrifugation, the flow-through was discarded, and the beads were carefully washed three times with strong RIPA lysis buffer and additional three times with PBS. The above beads were transferred to a new tube, followed by incubation with PBS containing 6 M urea and 10 mM dithiothreitol at 65 °C for 15 min. Iodoacetamide (IAA) was added to a final concentration of 20 mM and incubated for 40 min at room temperature in the dark. The beads were then washed twice with 0.02 M ammonium bicarbonate (ABC) and then resuspended in 0.02 M ABC, followed by the addition of trypsin at an enzyme-to-protein ratio of 1:25 (w/w). Cell surface fraction was digested on-bead at 37 °C overnight with gentle shaking. The digest was collected, followed by one wash with 3% formic acid (FA). Finally, the combined digest was acidified to 3% FA, lyophilized, and stored at –80 °C for subsequent reversed-phase liquid chromatography (RPLC)–MS/MS analysis.

**Amine-Reactive Cell Surface Biotinylation Method for Surfaceome Enrichment.** The HeLa surfaceome samples by amine-reactive cell surface biotinylation method was prepared as described with some modifications.<sup>23</sup> A brief description can be seen in the [Supporting Information](#).

**Western Blotting and Immunofluorescence Assay.** The details can be seen in the [Supporting Information](#).

**Nano-RPLC–Electrospray Ionization–MS/MS Analysis.** After protein digestion, the lyophilized peptides were resuspended in 0.1% FA/H<sub>2</sub>O solution and analyzed using a Dionex UltiMate 3000 RSLCnano system with a Q-Exactive mass spectrometer, controlled by Xcalibur software v 2.1.0 (Thermo Fisher Scientific, Waltham, MA, USA). The details can be seen in the [Supporting Information](#).

**Data Searching.** For protein identification, MS raw data files were analyzed using Proteome Discoverer (Thermo Scientific, v. 2.1.1.21) incorporated with mascot 2.5 (Matrix

Science Inc.) search engine. For the LFQ analysis, the raw data files were analyzed using the software MaxQuant v. 1.5.2.8 and then processed using Perseus software. The details can be seen in the [Supporting Information](#).

**Bioinformatic Analysis.** Protein cellular localization and statistical enrichment test were analyzed by PANTHER software (<http://pantherdb.org/>).<sup>24</sup> Proteins, which were unable to be mapped by PANTHER software, were then analyzed by UniProt database (<http://www.uniprot.org>) for the analysis of protein cellular localization. The software of TMHMM v. 2.0 (<http://www.cbs.dtu.dk/services/TMHMM/>) and Phobius (<http://phobius.sbc.su.se/>) were used to predict proteins with the transmembrane domains. Bioinformatics analysis was performed with Cytoscape, Perseus, and Microsoft Excel.

## RESULTS AND DISCUSSION

**Design of PECSL Technology for Surfaceome Profiling.** To label cell surface proteins, the labeling must be specific for the surface-exposed residues. For this purpose, biotin-xx-phenol probe (BxxP), which has a long and polar polyamide linker and was shown to be membrane-impermeable,<sup>21</sup> was chosen as the labeling probe in the PECSL strategy; HRP, which has four structurally essential disulfide bonds and is only active in the secretory pathway and extracellular environment, was chosen as the enzyme to catalyze the biotinylation of cell surface proteins in this work. Experimentally, living cells are first incubated with exogenous HRP and BxxP, followed by the addition of H<sub>2</sub>O<sub>2</sub> to start biotin labeling. In the presence of H<sub>2</sub>O<sub>2</sub>, peroxidase catalyzes the phenol residues on BxxP to undergo one-electron oxidation reaction and forms highly reactive and short-lived phenoxyl radicals, which could rapidly and covalently react with neighboring electron-rich amino acids, mostly Tyr, exposed on surface proteins.<sup>21</sup> The labeling reaction is allowed to continue for a short time and then quenched using ice-cold quenching buffer, which is a mixture of peroxidase inhibitors and a competitive substrate. In this way, only the proteins exposed on the living cell surface will be biotinylated. Afterward, the labeled cells are lysed and purified with avidin beads. The beads with the captured proteins are then resuspended in the chaotropic environment of 6 M urea for reduction and alkylation.<sup>25</sup> The utilization of a high concentration of chaotropic buffer could help the unfolding of hydrophobic cell surface proteins to facilitate efficient reduction and alkylation. Next, the beads are resuspended in ABC buffer for trypsin digestion on-bead.<sup>26,27</sup> The utilization of volatile buffer here allows the omit of the desalting step, which reduces sample loss and improves reproducibility. Finally, the cell surface protein digest is analyzed by LC–MS/MS ([Figure 1A](#)).

**PECSL Strategy Enables Efficient and Selective Cell Surface Protein Labeling within Seconds.** We first set out to test the efficiency and selectivity of the designed labeling strategy. PECSL labeling was performed for 1 min in living HeLa cells. For comparison, a negative control experiment, in which H<sub>2</sub>O<sub>2</sub> was omitted, was also performed to assess the endogenous biotinylation level. To investigate the efficiency of this labeling scheme, the above treated cells were lysed and analyzed by streptavidin-blot. As seen in [Figure 1B](#), the proteins in the experimental sample were efficiently biotinylated by the biotin-phenol reagent, and the biotinylation occurred in a H<sub>2</sub>O<sub>2</sub>-dependent manner. To investigate the selectivity of this labeling scheme, the above treated cells were

fixed and analyzed using confocal imaging of Alexa Fluor 568-labeled streptavidin. As seen in Figure 1C, the homogenous fluorescent labeling in the experimental group was only observed on the cell surface and extracellular space. Meanwhile, there were few intracellular dots with a slight fluorescence intensity from endogenous biotinylation in the negative group, which was consistent with our following MS proteomic results. These results demonstrated that the peroxidase-mediated labeling strategy could efficiently and selectively tag the cell surface proteins of living cells.

The designed HRP-mediated oxidative tyrosine coupling strategy is expected to have fast labeling kinetics for several reasons: (1) HRP is reported to have high catalytic activity<sup>28</sup> and phenoxyl radicals are highly reactive;<sup>29</sup> (2) without conjugation (like EMARS<sup>19</sup>) or gene fusion with target proteins (like APEX<sup>30</sup>), exogenous HRP has high activity; (3) in comparison with EMARS,<sup>19</sup> exogenous HRP allows to be worked at a higher concentration. For labeling kinetics assessment, we then evaluated the performance of PECSL technology for different labeling times by comparing with the conventional amine-reactive biotinylation method using streptavidin-blot and single-run LC-MS/MS measurement. The enzymatic biotin labeling ( $\sim 200 \mu\text{M}$  BxxP) and conventional amine-reactive cell surface labeling ( $\sim 411 \mu\text{M}$  sulfo-NHS-SS-biotin)<sup>23,31,32</sup> were performed for predetermined time points at room temperature in HeLa cells. As seen in Figures 1D,E, S1, S2 and Table S1, almost all samples by PECSL technology demonstrated significant biotinylation and consistent number of cell surface protein identification, except for a slight decrease of biotinylation for 10 s-PECSL-labeled sample, whereas the samples by amine-reactive labeling strategy demonstrated that the biotinylation was highly dependent on the labeling time, even when a higher concentration ( $\sim 1.65 \text{ mM}$ ) of sulfo-NHS-SS-biotin was utilized (Figure S1C–F). An average of 922 cell surface-annotated proteins were identified by 10 s-PECSL labeling, whereas only 454 cell surface-annotated proteins were identified by 10 s amine-reactive surface labeling. In addition, we found that distinct labeling patterns of streptavidin-blot were demonstrated for the two biotin labeling strategies (Figures 1D, S1C), which could be attributed to mainly the distinct sample loading buffers (with/without reducing reagents) and partly the different targeting residues. When a nonreducing sample loading buffer was employed for both strategies, similar labeling patterns were displayed in Figure S1D. In the meantime, given the above streptavidin-blot results, we also found that sulfo-NHS-SS-biotin labeling resulted in higher labeling efficiency than PECSL labeling with a prolonged labeling time, which could be attributed to the larger frequency of lysine than tyrosine in proteins (5.84 vs 2.92).<sup>33,34</sup> Overall, the above comparison demonstrated that the PECSL strategy has fast labeling kinetics and could be a powerful tool for the profiling of transient changes of the surfaceome with a high time resolution.

**PECSL Technology Allows Comprehensive Analysis of the HeLa Cell Surfaceome.** We further optimized the workflow for surfaceome profiling using western blotting and single-run LC-MS/MS measurement in HeLa cells (Figure S3 and Tables S2 and S3). The optimized workflow of PECSL technology was performed in HeLa cells with a labeling time of 1 min for four biological replicates. For recovery assessment, enriched peptides of each sample were resuspended in  $100 \mu\text{L}$  of 0.1% FA and analyzed by a NanoDrop 2000 spectropho-

tometer three times (Table S4). It was determined that  $7.9 \pm 0.17 \mu\text{g}$  ( $n = 4$ ) peptides were enriched by PECSL technology from  $\sim 1 \text{ mg}$  labeled HeLa cell samples. Next, each sample was analyzed by LC-MS/MS with one technical run. In total, 2684 proteins (“PECSL data”) were identified from the four biological replicates, of which, 1370 (51%) proteins were classified as the cell surface/plasma membrane/extracellular proteins (cell surface-annotated proteins) and 862 (32%) proteins were classified as plasma membrane proteins (cell surface/plasma membrane) by gene ontology (GO) annotation<sup>23,35</sup> (Table S5).

Theoretically, given the result of immunofluorescence analysis (Figure 1C), proteins exposed on the cell surface could be biotinylated, highly enriched on avidin beads, digested on-bead, and identified by LC-MS/MS. In the meantime, noncell surface proteins could be reduced or completely removed. To evaluate the surfaceome enrichment efficiency, we first comprehensively compared the PECSL data with the global proteomic data, where total HeLa cell lysates from four biological replicates were analyzed (Table S5). As seen in Figure 2A and Table S5, sequence coverage and peptide spectrum match (PSM), which could reflect the protein abundance, for many high-confidence cell surface proteins have been greatly improved in the PECSL data. For example, the number of spectra count for EGFR, an important receptor protein on the cell surface, increased by about 18-folds (375 vs 21), and its sequence coverage also increased by about 4.4-folds (57 vs 13). Out of the 156 high-abundance proteins (PSMs  $\geq 100$ ) in the PECSL data, 132 (84.6%) were annotated as cell surface proteins, and additional 6 (3.8%) were biotin metabolic process-related proteins by GO annotation. Furthermore, 15 out of the remaining 18 noncell surface proteins were annotated as “membrane” by UniProtKB/Swiss-Prot. The above results indicated that high-abundance proteins (e.g., high numbers of PSMs) are more likely to be bona fide cell surface proteins. To further confirm the specificity of this method, the GO enrichment analysis was then conducted by using the global proteomic data as the reference list. As seen in Figure 2B and Table S6, cell surface-related GO terms, including “cell surface,” “plasma membrane,” “receptor complex,” and “integral component of membrane” were significantly enriched in the PECSL data, demonstrating the effectiveness of PECSL technology for surfaceome enrichment. The number of transmembrane proteins (TMPs) and cluster of differentiation (CD) antigens were also analyzed. Seven hundred and thirty two out of 2684 (27.3%) in the PECSL data and 549 out of 3510 (15.6%) in the global proteomic data were predicted to be TMPs (Figure S4, Table S5). Highly hydrophobic TMPs with  $>5$  transmembrane domains (TMDs) were much more enriched in the PECSL data compared with the global proteomic data (126 vs 70). The number of CD antigens in the PECSL data (81 CD antigens, corresponding to 84 cell surface proteins) increased by about 2-folds compared with that in the global proteomic data (41 CD antigens, corresponding to 43 cell surface proteins). The above results further confirmed that the surfaceome was highly enriched by this new labeling strategy.

To further confirm the performance of PECSL technology, GenieScore,<sup>36</sup> where four previous bioinformatics-based constructions of the human cell surface proteome of 5407 proteins were compiled for a consensus-based prediction of cell surface localization, was utilized to analyze the PECSL data and multiple surfaceome data generated by using different

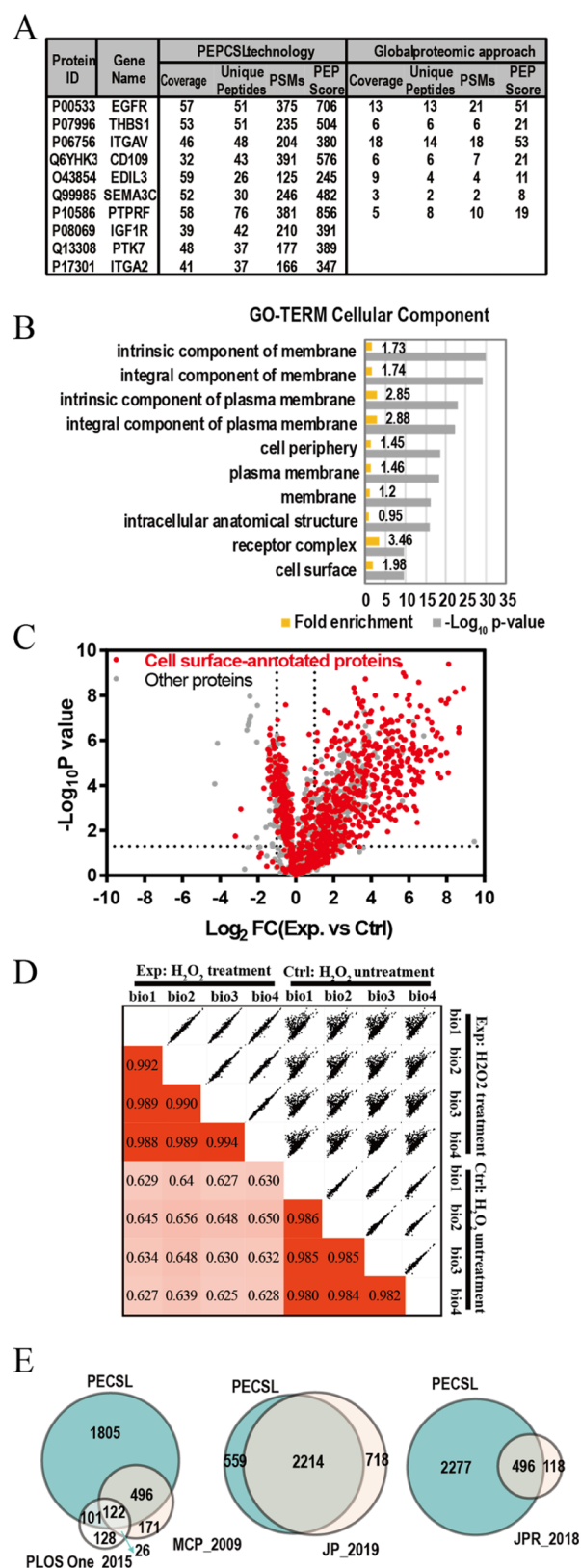


**Figure 2.** PECSL technology allows comprehensive analysis of the HeLa cell surfaceome. Four biological replicates were performed for PECSL technology and global proteomic approach in HeLa cells, and each replicate was analyzed with one technical run. (A) Sequence coverage and spectra count of multiple high-confidence cell surface proteins were analyzed for the PECSL data and global proteomic data. The details can be seen in Table S5. (B) GO enrichment analysis according to cellular component was performed for the PECSL data,

**Figure 2.** continued

and the global proteomic data was set as the reference gene list. Gray bars illustrate the significance threshold, and the top 10 protein groups are displayed. The details also can be seen in Table S6. (C) Comparison of the pull-down proteins between the control (without  $H_2O_2$  treatment) and experimental ( $H_2O_2$  treatment for 1 min) cell samples by the LFQ method. Fold change ( $x$ -axis) is shown as  $\log_2$ ;  $p$ -value, which was calculated using the software of Perseus, is shown as  $-\log_{10}$ . Red dots localize to cell surface/plasma membrane/extracellular by GO annotation. Details can be seen in Table S7. (D) LFQ value for each biological replicate was plotted against each other replicate for reproducibility assessment. (E) Comparison of the PECSL data with multiple previous HeLa surfaceome data generated by using different enrichment strategies (left,<sup>39,44</sup> middle,<sup>23</sup> right<sup>13</sup>).

enrichment strategies. As seen in Table S7, in terms of the number of identified likely cell surface proteins, which have a surface prediction consensus (SPC) score larger than 0), PECSL technology (713), lysine-targeting methods (202–734), and sucrose density gradient centrifugation method (816–1631) outperform the glycan chain method (180–436) and carboxyl group method (208). As for the highly likely cell surface proteins (SPC score 3, 4), PECSL technology (11.3%) has a similar specificity compared with lysine-targeting methods (10.1–26.7%) and sucrose density gradient centrifugation method (7.8–13.1%)<sup>13,23,37,38</sup> and a lower specificity than glycan chain-targeting methods (14.2–69.3%) and carboxyl group-targeting method (49.5%),<sup>13,37,39,40</sup> but a much higher specificity than the whole cell lysate data (3.4%) with SurfaceGenie. It reminded us that as previous studies reported,<sup>38,41–43</sup> many noncell surface proteins were also copurified through strong interactions with highly hydrophobic cell surface proteins or avidin-affinity material. To determine which proteins are truly present on the cell surface, an LFQ proteomics experiment was employed to compare the enriched proteins between the control and experimental cell samples. Negative control cell samples, in which  $H_2O_2$  was removed from the PECSL labeling buffer, were prepared along with the experimental groups during all experimental procedures. As seen in Figure 2C and Table S8, after data filtering, a total of 1757 proteins, including 979 cell surface-annotated proteins, were quantified and 731 proteins were significantly enriched ( $p$ -value  $< 0.05$ ,  $\geq 2$ -fold) in the  $H_2O_2$ -treated experimental groups. Out of the 731 proteins, 500 (68%) were classified as cell surface proteins by GO annotation and 202 (27.6%) proteins were highly likely cell surface proteins (SPC score 3, 4) with SurfaceGenie. In addition, the more stringent the filter criteria were set, higher specificity of PECSL technology was observed. For example, out of 321 significantly enriched proteins ( $p$ -value  $< 0.05$ ,  $\geq 8$ -fold), 270 (84%) were classified as cell surface proteins by GO annotation and 145 (45.2%) were highly likely cell surface proteins with SurfaceGenie. In this case, the proteins quantified with a larger fold change are more likely to be bona fide cell surface proteins. Nevertheless, for a specific protein, further validation experiment is required. Finally, LFQ values for each technical run were plotted against each other replicate using Perseus software for reproducibility assessment (Figure 2D). Consistent with western blotting analysis (Figure S5), the four biological replicates resulted in a high Pearson correlation coefficient (average  $R^2 = 0.99$ ), demonstrating high reproducibility of the workflow of the PECSL technology.

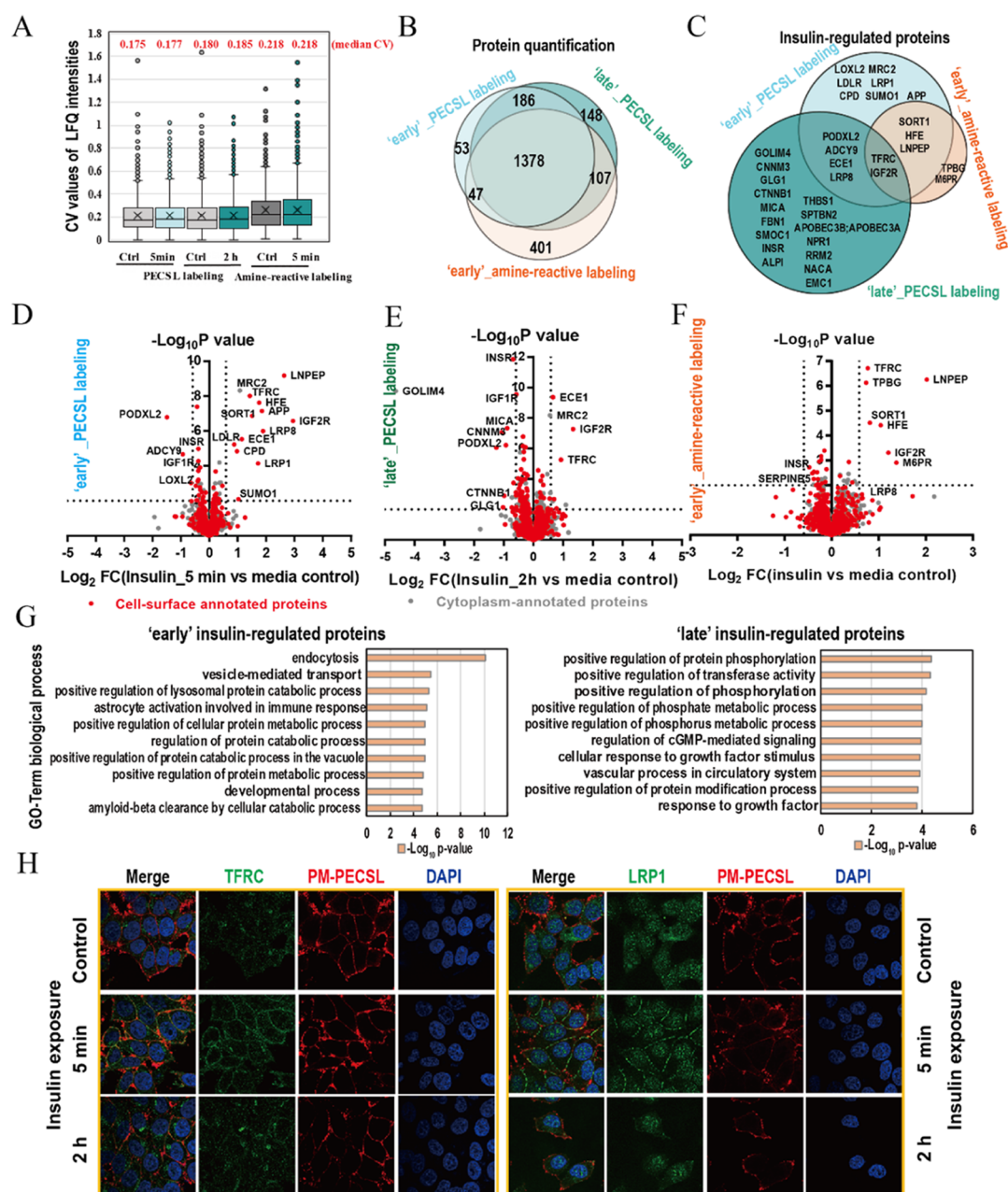


**Figure 3.** Temporal surfaceome profiling after insulin exposure for 5 min and 2 h in HepG2 cells. Three biological replicates of each time point were performed, and three LC–MS/MS runs were performed for each sample. (A) CV values for each time-point sample were analyzed on the protein level. (B) Venn diagram for the quantified proteins in the two time-point experiment. (C) Venn diagram for the insulin-regulated proteins after insulin treatment for 5 min or 2 h by PECSL technology and amine-reactive cell surface biotinylation. (D–F) Volcano plots show the surfaceome quantification results comparing insulin treatment for 5 min (“early”) or 2 h (“late”) and media control groups (FDR < 0.01). Fold change ( $x$ -axis) is shown as  $\log_2$ ;  $p$ -value, which was calculated using the software of Perseus, is shown as  $-\log_{10}$ . Red dots are cell surface/plasma membrane/extracellular by GO annotation. (G) GO enrichment analysis according to the biological process was performed for the “early” (5 min) and “late” (2 h) insulin-regulated proteins, and the top 10 protein groups are displayed. The details can be seen in Table S10. (H) Verification of the dynamic abundance changes of the two insulin-regulated proteins, TFRC and LRP, after insulin exposure using the immunofluorescence assay.

In the recent decade, chemical labeling-based methods have been powerful tools for surfaceome profiling.<sup>1</sup> To date, most chemical-labeling probes selectively target surface-exposed Lys, Asp, Glu, Cys, or glycosylated side chains. Here, PECSL technology mainly targets the surface-exposed tyrosine residues. To evaluate the surfaceome mapping capacity, we then compared our PECSL data with multiple HeLa surfaceome data generated by using different enrichment strategies. Taking advantage of the fact that nearly all cell surface proteins ( $\sim 90\%$ ) are glycosylated in vertebrates,<sup>5</sup>

several cell surface glycoprotein enrichment strategies have been established and applied to profile the HeLa surfaceome.<sup>1</sup> We first compared the PECSL data with two published HeLa surface glycoproteomic data. As seen in Figure 2E (left), our PECSL data could cover about 65% (244/377) of cell surface proteins identified by CSC technology<sup>44</sup> and about 72% (589/815) of total cell surface proteins identified by both lectin-affinity purification and glyco-capture approaches.<sup>39</sup> It should be noted that our PECSL data (1370) allowed the identification of about 3.6- and 1.7-fold more cell surface-

annotated proteins. We recently profiled the HeLa surfaceome by an optimized amine-reactive cell surface biotinylation method,<sup>23</sup> and the identification result was then compared with the PECSL data. We found that about 72% (2102/2932) of the amine-reactive cell surface biotinylation data were also covered by the PECSL data (Figure 2E, middle). Very recently, Özlü et al. performed both carboxyl-reactive and amine-reactive cell surface biotinylation methods to profile the HeLa surfaceome,<sup>13</sup> and our PECSL data could cover about 82% (504/614) of their total identifications (Figure 2E, right). The above results confirmed the good coverage in the surfaceome by the PECSL technology.

In summary, with a labeling time of 1 min, 2684 proteins, including 1370 (51%) cell surface-annotated proteins, 732 TMPs, and 81 CD antigens, were identified from  $4 \times 10^6$  HeLa cells by the PECSL technology. By comparison with the negative control experiment using quantitative proteomics, higher specificity was achieved and 500 (68%) out of the 731 significantly enriched proteins ( $p$ -value < 0.05,  $\geq 2$ -fold) in positive experimental samples were cell surface-annotated proteins. By comparison with the global proteomic data and multiple HeLa surfaceome data, we found that the PECSL data allows selective HeLa cell surfaceome profiling with good reproducibility and coverage.

**Temporal Profiling of the Surfaceome after Insulin Exposure for 5 min and 2 h in HepG2 Cells.** We then asked if the PECSL technology could give a specific “snapshot” of the temporal dynamic changes of the surfaceome by tracking of insulin action on the plasma membrane in a human liver cancer cell line, HepG2 cells. The mechanism of insulin action is a central theme in biology, and a better understanding of insulin signaling could help the discovery of new disease treatment modalities, such as type 2 diabetes, obesity, insulin resistance, hypertension, Alzheimer disease, and cancer.<sup>45</sup> As a general rule, upon insulin binding, insulin receptor tyrosine kinases undergo auto-phosphorylation, followed by triggering downstream signaling events. The transmission of the insulin receptor signal to its various mediators occurs over varying lengths of time, resulting in temporal dynamics of diverse biological processes, including growth, differentiation, mobility, and glucose homeostasis.<sup>46</sup>

A two time-point experiment was performed to explore the temporal dynamic changes of the surfaceome after insulin exposure for 5 min and 2 h. In the experiment, serum-starved HepG2 cells were treated with 37 °C prewarmed media containing 200 nM insulin at 37 °C for 5 min or 2 h, and meanwhile, cell samples treated with the same volume of 37 °C prewarmed insulin-free media were also prepared as controls to assess the abundance changes of biotinylated proteins upon insulin treatment. After PBS washing, PECSL labeling was performed for 1 min at room temperature. In comparison, amine-reactive cell surface biotinylation method was also performed to monitor the surfaceome changes after insulin treatment for 5 min. Three biological replicates for each time point were performed, and three LC–MS/MS runs were performed for each sample. LFQ method was employed to quantify the relative abundance changes of biotinylated proteins following insulin exposure. For reproducibility assessment, coefficient of variation (CV) values of each time-point sample were analyzed on protein level. As seen in Figure 3A, with a slightly smaller CV value (median 0.176 vs 0.218), PECSL technology demonstrated better reproducibility than the amine-reactive cell surface biotinylation method.

Finally, after data filtering (details can be seen in the Supporting Information), totally, 1664 and 1819 proteins were quantified with 882 cell surface-annotated proteins (red dots) from the two time points by PECSL technology (Figure 3B, Table S9), out of which, 16 and 22 proteins (totally 32) were found to be significantly regulated after insulin exposure for 5 min and 2 h, respectively (Figure 3C–E,  $p$ -value < 0.01,  $\geq 1.5$ -fold). In comparison, 1933 proteins were quantified with 965 cell surface-annotated proteins (red dots) by the amine-reactive cell surface biotinylation method (Figure 3B, Table S9), out of which, 7 proteins (Figure 3C,F,  $p$ -value < 0.01,  $\geq 1.5$ -fold) were found to be significantly regulated after insulin exposure for 5 min. Majority (>70%) of the quantified proteins by both the methods were overlapped (Figure 3B). In addition, 14 out of the 16 “early” insulin-regulated proteins quantified by PECSL technology were also identified by the amine-reactive cell surface biotinylation method but demonstrated no significant ( $p$ -value < 0.01) abundance changes (Table S9). Immediately after insulin stimulation, the abundances of several proteins were found to have a quick increase (5 min) on the cell surface and then decreased with prolonged insulin treatment (2 h) (Figure S6). TFRC, IGF2R,<sup>47</sup> LNPEP,<sup>48</sup> SORT1,<sup>49</sup> and LRP1<sup>50</sup> are associated with the trafficking of glucose transporter 4 (GLUT4) storage vesicles. Upon insulin binding to its surface receptors, it immediately undergoes receptor-mediated endocytosis; in seconds, the downstream of AKT is activated for the quick translocation of GLUT4 vesicles onto cell surface for growing,<sup>51,52</sup> which could explain acute dynamic abundance changes on the plasma membrane of GLUT4-associated proteins upon insulin exposure in the LFQ data by PECSL technology and amine-reactive cell surface biotinylation method. In addition, the LFQ data by PECSL technology additionally detected a quick abundance increase on the plasma membrane of several insulin-regulated proteins after insulin exposure for 5 min, such as LDLR, ECE1, APP, CPD, LRP8, and MRC2 (Figure S6). LDLR has been reported to be associated with rapid endocytosis of extracellular macromolecules and have a rapid abundance increase on the cell surface with LRP1 upon insulin binding;<sup>50,53</sup> ECE1 has been reported to be involved in the hydrolysis of peptide hormones, including insulin and A $\beta$ ,<sup>54–56</sup> CPD has been reported to function as a receptor to be recycled from the cell surface to the trans-Golgi network, and its homologue silver has been reported to regulate memory formation via the insulin pathway in *Drosophila*.<sup>57–59</sup> These proteins probably also involve in the trafficking of GLUT4 storage vesicles. To further confirm the hypothesis, string analysis was then performed to illustrate known and predicted functional interactions within “early” and “late” insulin-regulated proteins by the software Cytoscape (Figure S7), and a closer interaction network was observed for the “early” insulin-regulated proteins of ADCY9, APP, LRP8, ECE1, LRP1, SORT1, LNPEP, LDLR, IGF2R, TFRC, CPD, and HFE. Besides, abundances of several proteins were found to have a decrease on the plasma membrane of HepG2 cells upon insulin exposure, including INSR, PODXL2, ADCY9, MICA, CNNM3, GOLIM4, GLG1, PCNT and so forth (Figure S6). Upon insulin binding, the ligand-mediated receptor undergoes endocytosis, and insulin receptor proteins of INSR and IGF1R are internalized into endocytic vesicles, sorted into early endosomes, and either targeted in the lysosomes for degradation or recycled to the plasma membrane,<sup>60–62</sup> which could explain the sustained abundance decrease of INSR and IGF1R on the cell surface

after insulin treatment. A rapid and substantial decrease was observed for the cell surface-annotated proteins PODXL2 and ADCY9, whereas the abundance of GOLIM4, CNNM3, and GLG1 was observed to be significantly decreased only with prolonged insulin treatment (2 h). These observations suggest that our methodology has sufficient temporal resolution to detect transient changes of the surfaceome. We then conducted biological process classification for the “early” (5 min) and “late” (2 h) insulin-regulated proteins. Not surprisingly, the biological processes of “endocytosis,” “vesicle-mediated transport,” and “developmental process” were significantly enriched ( $p$ -value < 0.0001) in the transient insulin-regulated proteins, whereas “positive regulation of protein phosphorylation,” “regulation of cGMP-mediated signaling,” and “cellular response to growth factor stimulus” were significantly enriched ( $p$ -value < 0.001) in the long-term insulin-regulated proteins (Figure 3G, Table S10). Upon insulin exposure, cell surface proteins undergo changing interaction networks and dynamic translation because of extensive trafficking between the plasma membrane and the endomembrane compartment via exocytosis, endocytosis, and recycling processes.<sup>51</sup> With prolonged insulin exposure, diverse intercellular signaling was then selectively activated by the regulation (mostly phosphorylation) of downstream molecules. We finally verified the dynamic abundance changes of LRP1 and TFRC after insulin treatment for 5 min and 2 h using the immunofluorescence assay (Figure 3H), which was consistent with our LFQ data. The above results indicated that many cell surface proteins are indeed highly dynamic in response to insulin stimulation, and PECSL technology coupled with the LFQ method has sufficient resolution to detect transient changes of the surfaceome.

## CONCLUSIONS

It is well known that proteins on the cell surface change rapidly to adapt to the environment. To get a better understanding of cellular physiology and decipher the complex cellular processes, global profiling of the dynamic changes of the surfaceome with a high time resolution is necessary but remains challenging. In this work, we reported a fast cell surface labelling strategy, termed as PECSL, to efficiently label cell surface proteins within seconds. By combining with affinity purification, on-bead digestion, and LC-MS/MS measurement, PECSL technology demonstrated efficient and selective surfaceome profiling with high reproducibility. This technology coupled with the LFQ method was applied to profile dynamic changes of the surfaceome after insulin treatment at two time points, 5 min and 2 h. In comparison with the conventional amine-reactive cell surface biotinylation method, more insulin-regulated proteins were revealed after insulin treatment for 5 min by PECSL technology (16 vs 7), demonstrating that our methodology has sufficient temporal resolution to detect transient changes of the surfaceome.

It should be noted that there are some limitations for the current PECSL technology. On the one hand, cell surface proteins may not be detected by PECSL technology due to lack of available reactive moieties, mainly tyrosine residues, exposed on the protein extracellular sequence. On the other hand, as mentioned above, many noncell surface proteins were still identified in our PECSL data, which could be derived from the labeling step and sample preparation steps. For higher specificity, except for comparing with parallel negative control groups (Figure 2C), keeping the living cells in good condition,

boiling the cell lysates for a short while before affinity purification, washing with harsh buffers during affinity purification, lysing with hypotonic buffer for prior enrichment by ultracentrifugation method, and/or washing the cell debris with alkaline carbonate buffer could help reduce the cytoplasmic contaminations. In addition, the introduction of a cleavable residue in the linker of the labeling reagent could not only help the elution of cell surface proteins and the identification of labeled peptides but also help reduce the contaminations from affinity materials.

With the continuing improvements of PECSL technology, we believe it could serve as a powerful tool to track the transient changes of the surfaceome with a good time resolution and help delineate the function and regulatory mechanisms of the highly dynamical cellular signaling involving cell surface proteins.

## ASSOCIATED CONTENT

### Supporting Information

The Supporting Information is available free of charge at <https://pubs.acs.org/doi/10.1021/acs.analchem.0c04970>.

Reagents and materials, supplementary methods, evaluation of biotinylation performance of PECSL technology and amine-reactive cell surface labeling for different labeling times, and workflow optimization of PECSL technology for HeLa cell surfaceome profiling (PDF)

Identification information of HeLa surfaceome data by PECSL labeling and amine-reactive cell surface labeling with different labeling times (XLSX)

LFQ information for the pulldown proteins between the control (without BxxP) and experimental (~200  $\mu$ M BxxP) cell samples and GO enrichment analysis for the up-regulated proteins ( $p$ -value < 0.05,  $\geq$  2-fold) of the pulldown samples in the experimental versus control (without BxxP) groups (XLSX)

LFQ information for whole lysate proteins between the control (without H<sub>2</sub>O<sub>2</sub>) and experimental (1 mM H<sub>2</sub>O<sub>2</sub>) group cell samples and string analysis for the up-regulated proteins ( $p$ -value < 0.05,  $\geq$  2-fold) of whole lysate samples in the experimental versus control (without H<sub>2</sub>O<sub>2</sub>) groups (XLSX)

List of proteins identified by PECSL technology and global proteomic approach (XLSX)

GO enrichment analysis performed for the PECSL data according to cellular component and proteins identified by the global proteomic approach set as the reference gene list (XLSX)

LFQ information for the enriched proteins between the experimental and control (without H<sub>2</sub>O<sub>2</sub> treatment) cell samples (XLSX)

Surfaceome quantification information by PECSL technology and amine-reactive cell surface biotinylation method after insulin treatment (XLSX)

GO enrichment analysis of “early” (5 min) and “late” (2 h) insulin-regulated proteins according to biological process (XLSX)

## AUTHOR INFORMATION

### Corresponding Author

Mingliang Ye – CAS Key Laboratory of Separation Science for Analytical Chemistry, Dalian Institute of Chemical Physics, Chinese Academy of Sciences (CAS), Dalian 116023, China;

orcid.org/0000-0002-5872-9326; Phone: +86-411-84379610; Email: mingliang@dicp.ac.cn; Fax: +86-411-84379620

## Authors

**Yanan Li** – CAS Key Laboratory of Separation Science for Analytical Chemistry, Dalian Institute of Chemical Physics, Chinese Academy of Sciences (CAS), Dalian 116023, China

**Yan Wang** – CAS Key Laboratory of Separation Science for Analytical Chemistry, Dalian Institute of Chemical Physics, Chinese Academy of Sciences (CAS), Dalian 116023, China; University of Chinese Academy of Sciences, Beijing 100049, China

**Yating Yao** – CAS Key Laboratory of Separation Science for Analytical Chemistry, Dalian Institute of Chemical Physics, Chinese Academy of Sciences (CAS), Dalian 116023, China

**Jiawen Lyu** – CAS Key Laboratory of Separation Science for Analytical Chemistry, Dalian Institute of Chemical Physics, Chinese Academy of Sciences (CAS), Dalian 116023, China; University of Chinese Academy of Sciences, Beijing 100049, China; orcid.org/0000-0001-9641-685X

**Qinglong Qiao** – CAS Key Laboratory of Separation Science for Analytical Chemistry, Dalian Institute of Chemical Physics, Chinese Academy of Sciences (CAS), Dalian 116023, China

**Jiawei Mao** – CAS Key Laboratory of Separation Science for Analytical Chemistry, Dalian Institute of Chemical Physics, Chinese Academy of Sciences (CAS), Dalian 116023, China

**Zhaochao Xu** – CAS Key Laboratory of Separation Science for Analytical Chemistry, Dalian Institute of Chemical Physics, Chinese Academy of Sciences (CAS), Dalian 116023, China; orcid.org/0000-0002-2491-8938

Complete contact information is available at:  
<https://pubs.acs.org/10.1021/acs.analchem.0c04970>

## Notes

The authors declare no competing financial interest. The raw data was uploaded onto JPOST Repository.<sup>63</sup> The accession numbers are PXD022744 for ProteomeXchange and JPST001019 for jPOST.

## ACKNOWLEDGMENTS

This work was supported, in part, by funds from the National Key Research and Development Program of China (2016YFA0501402 and 2017YFA0505003), the National Natural Science Foundation of China (21535008, 81730016, and 91753105), Liaoning Revitalization Talents Program, the innovation program (DICP&QIBEBT UN201802 and DICP I201935) of science and research from the DICP, CAS, and Innovation Academy for Precision Measurement Science and Technology, CAS. M.Y. is a recipient of the National Science Fund of China for Distinguished Young Scholars (21525524).

## REFERENCES

- (1) Li, Y.; Qin, H.; Ye, M. *J. Sep. Sci.* **2020**, *43*, 292–312.
- (2) Hurlley, W. L.; Finkelstein, E.; Holst, B. D. *J. Immunol. Methods* **1985**, *85*, 195–202.
- (3) Rybak, J.-N.; Ettore, A.; Kaissling, B.; Giavazzi, R.; Neri, D.; Elia, G. *Nat. Methods* **2005**, *2*, 291–298.
- (4) Wollscheid, B.; Bausch-Fluck, D.; Henderson, C.; O'Brien, R.; Bibel, M.; Schiess, R.; Aebersold, R.; Watts, J. D. *Nat. Biotechnol.* **2009**, *27*, 378–386.

- (5) Boheler, K. R.; Gundry, R. L. *Stem Cells Transl. Med.* **2017**, *6*, 131–138.
- (6) Kalxdorf, M.; Gade, S.; Eberl, H. C.; Bantscheff, M. *Mol. Cell. Proteomics* **2017**, *16*, 770–785.
- (7) Yoon, C.; Song, H.; Yin, T.; Bausch-Fluck, D.; Frei, A. P.; Kattman, S.; Dubois, N.; Witty, A. D.; Hewel, J. A.; Guo, H.; Emili, A.; Wollscheid, B.; Keller, G.; Zandstra, P. W. *Stem Cell Rep.* **2018**, *10*, 87–100.
- (8) Leung, K. K.; Nguyen, A.; Shi, T.; Tang, L.; Ni, X.; Escoubet, L.; MacBeth, K. J.; DiMartino, J.; Wells, J. A. *Proc. Natl. Acad. Sci. U.S.A.* **2019**, *116*, 695–700.
- (9) Heinzlmann, K.; Noskovičová, N.; Merl-Pham, J.; Preissler, G.; Winter, H.; Lindner, M.; Hatz, R.; Hauck, S. M.; Behr, J.; Eickelberg, O. *Int. J. Biochem. Cell Biol.* **2016**, *74*, 44–59.
- (10) Béguin, E. P.; van den Eshof, B. L.; Hoogendijk, A. J.; Nota, B.; Mertens, K.; Meijer, A. B.; van den Biggelaar, M. J. *Proteomics* **2019**, *19*, 89–101.
- (11) Miki, Y.; Takahashi, D.; Kawamura, Y.; Uemura, M. *J. Proteomics* **2019**, *197*, 71–81.
- (12) Zeng, Y.; Ramya, T. N. C.; Dirksen, A.; Dawson, P. E.; Paulson, J. C. *Nat. Methods* **2009**, *6*, 207–209.
- (13) Özkan Küçük, N. E.; Şanal, E.; Tan, E.; Mitchison, T.; Özlü, N. *J. Proteome Res.* **2018**, *17*, 1784–1793.
- (14) Wu, Y.; Wu, S.; Ma, S.; Yan, F.; Weng, Z. *Anal. Chem.* **2019**, *91*, 3187–3194.
- (15) Ross, E.; Ata, R.; Thavarajah, T.; Medvedev, S.; Bowden, P.; Marshall, J. G.; Antonescu, C. N. *PLoS One* **2015**, *10*, No. e0128013.
- (16) Moche, M.; Schlüter, R.; Bernhardt, J.; Plate, K.; Riedel, K.; Hecker, M.; Becher, D. *J. Proteome Res.* **2015**, *14*, 3804–3822.
- (17) Bobrow, M. N.; Harris, T. D.; Shaughnessy, K. J.; Litt, G. J. *J. Immunol. Methods* **1989**, *125*, 279–285.
- (18) Bar, D. Z.; Atkash, K.; Tavarez, U.; Erdos, M. R.; Gruenbaum, Y.; Collins, F. S. *Nat. Methods* **2018**, *15*, 127–133.
- (19) Kotani, N.; Gu, J.; Isaji, T.; Udaka, K.; Taniguchi, N.; Honke, K. *Proc. Natl. Acad. Sci. U.S.A.* **2008**, *105*, 7405–7409.
- (20) Li, X.-W.; Rees, J. S.; Xue, P.; Zhang, H.; Hamaia, S. W.; Sanderson, B.; Funk, P. E.; Farndale, R. W.; Lilley, K. S.; Perrett, S.; Jackson, A. P. *J. Biol. Chem.* **2014**, *289*, 14434–14447.
- (21) Loh, K. H.; Stawski, P. S.; Draycott, A. S.; Udeshi, N. D.; Lehrman, E. K.; Wilton, D. K.; Svinkina, T.; Deerinck, T. J.; Ellisman, M. H.; Stevens, B.; Carr, S. A.; Ting, A. Y. *Cell* **2016**, *166*, 1295–1307.
- (22) Li, J.; Han, S.; Li, H.; Udeshi, N. D.; Svinkina, T.; Mani, D. R.; Xu, C.; Guajardo, R.; Xie, Q.; Li, T.; Luginbuhl, D. J.; Wu, B.; McLaughlin, C. N.; Xie, A.; Kaewsapsak, P.; Quake, S. R.; Carr, S. A.; Ting, A. Y.; Luo, L. *Cell* **2020**, *180*, 373–386.
- (23) Li, Y.; Wang, Y.; Mao, J.; Yao, Y.; Wang, K.; Qiao, Q.; Fang, Z.; Ye, M. *J. Proteomics* **2019**, *196*, 33–41.
- (24) Mi, H.; Muruganujan, A.; Casagrande, J. T.; Thomas, P. D. *Nat. Protoc.* **2013**, *8*, 1551–1566.
- (25) Qin, W.; Lv, P.; Fan, X.; Quan, B.; Zhu, Y.; Qin, K.; Chen, Y.; Wang, C.; Chen, X. *Proc. Natl. Acad. Sci. U.S.A.* **2017**, *114*, E6749–E6758.
- (26) Dormeyer, W.; van Hoof, D.; Mummery, C. L.; Krijgsvelde, J.; Heck, A. J. R. *Proteomics* **2008**, *8*, 4036–4053.
- (27) Wiśniewski, J. R.; Zougman, A.; Nagaraj, N.; Mann, M. *Nat. Methods* **2009**, *6*, 359–362.
- (28) Han, S.; Li, J.; Ting, A. Y. *Curr. Opin. Neurobiol.* **2018**, *50*, 17–23.
- (29) Mortensen, A.; Skibsted, L. H. *J. Agric. Food Chem.* **1997**, *45*, 2970–2977.
- (30) Paek, J.; Kalocsay, M.; Staus, D. P.; Wingler, L.; Pascolutti, R.; Paulo, J. A.; Gygi, S. P.; Kruse, A. C. *Cell* **2017**, *169*, 338–349.
- (31) Elia, G. *Methods Mol. Biol.* **2019**, *1855*, 449–459.
- (32) Kasvandik, S.; Sillaste, G.; Velthut-Meikas, A.; Mikelsaar, A.-V.; Hallap, T.; Padrik, P.; Tenson, T.; Jaakma, Ü.; Kõks, S.; Salumets, A. *Proteomics* **2015**, *15*, 1906–1920.
- (33) Cedano, J.; Aloy, P.; Pérez-Pons, J. A.; Querol, E. *J. Mol. Biol.* **1997**, *266*, 594–600.

- (34) Nakashima, H.; Nishikawa, K. *FEBS Lett.* **1992**, *303*, 141–146.
- (35) Özlü, N.; Qureshi, M. H.; Toyoda, Y.; Renard, B. Y.; Mollaoglu, G.; Özkan, N. E.; Bulbul, S.; Poser, I.; Timm, W.; Hyman, A. A.; Mitchison, T. J.; Steen, J. A. *EMBO J.* **2015**, *34*, 251–265.
- (36) Waas, M.; Snarrenberg, S. T.; Littrell, J.; Jones Lipinski, R. A.; Hansen, P. A.; Corbett, J. A.; Gundry, R. L. *Bioinformatics* **2020**, *36*, 3447–3456.
- (37) Nagano, K.; Shinkawa, T.; Kato, K.; Inomata, N.; Yabuki, N.; Haramura, M. *J. Proteomics* **2011**, *74*, 1985–1993.
- (38) Akdag, M.; Yunt, Z. S.; Kamacioglu, A.; Qureshi, M. H.; Akarlar, B. A.; Ozlu, N. *J. Proteome Res.* **2020**, *19*, 3583–3592.
- (39) McDonald, C. A.; Yang, J. Y.; Marathe, V.; Yen, T. Y.; BA, M. *Mol. Cell. Proteomics* **2009**, *8*, 287–301.
- (40) Sun, F.; Suttapitugsakul, S.; Wu, R. *Anal. Chem.* **2019**, *91*, 4195–4203.
- (41) Karhemo, P.-R.; Ravela, S.; Laakso, M.; Ritamo, I.; Tatti, O.; Mäkinen, S.; Goodison, S.; Stenman, U.-H.; Hölttä, E.; Hautaniemi, S.; Valmu, L.; Lehti, K.; Laakkonen, P. *J. Proteomics* **2012**, *77*, 87–100.
- (42) Hörmann, K.; Stukalov, A.; Müller, A. C.; Heinz, L. X.; Superti-Furga, G.; Colinge, J.; Bennett, K. L. *J. Proteome Res.* **2016**, *15*, 647–658.
- (43) Pribyl, T.; Moche, M.; Dreisbach, A.; Bijlsma, J. J. E.; Saleh, M.; Abdullah, M. R.; Hecker, M.; van Dijk, J. M.; Becher, D.; Hammerschmidt, S. *J. Proteome Res.* **2014**, *13*, 650–667.
- (44) Bausch-Fluck, D.; Hofmann, A.; Bock, T.; Frei, A. P.; Cerciello, F.; Jacobs, A.; Moest, H.; Omasits, U.; Gundry, R. L.; Yoon, C.; Schiess, R.; Schmidt, A.; Mirkowska, P.; Hartlova, A.; Van Eyk, J. E.; Bourquin, J. P.; Aebersold, R.; Boheler, K. R.; Zandstra, P.; Wollscheid, B. *PLoS One* **2015**, *10*, No. e0121314.
- (45) Haeusler, R. A.; McGraw, T. E.; Accili, D. *Nat. Rev. Mol. Cell Biol.* **2018**, *19*, 31–44.
- (46) Kubota, H.; Noguchi, R.; Toyoshima, Y.; Ozaki, Y.-i.; Uda, S.; Watanabe, K.; Ogawa, W.; Kuroda, S. *Mol. Cell* **2012**, *46*, 820–832.
- (47) Braulke, T. *Horm. Metab. Res.* **1999**, *31*, 242–246.
- (48) Demaegdt, H.; Smits, L.; De Backer, J.-P.; Le, M. T.; Bauwens, M.; Szemenyei, E.; Tóth, G.; Michotte, Y.; Vanderheyden, P.; Vauquelin, G. *Br. J. Pharmacol.* **2008**, *154*, 872–881.
- (49) Shi, J.; Kandrór, K. V. *Dev. Cell* **2005**, *9*, 99–108.
- (50) Laatsch, A.; Merkel, M.; Talmud, P. J.; Grewal, T.; Beisiegel, U.; Heeren, J. *Atherosclerosis* **2009**, *204*, 105–111.
- (51) Foley, K.; Boguslavsky, S.; Klip, A. *Biochemistry* **2011**, *50*, 3048–3061.
- (52) Kioumourtoglou, D.; Pryor, P. R.; Gould, G. W.; Bryant, N. J. *J. Cell Sci.* **2015**, *128*, 2423–2429.
- (53) Ramakrishnan, G.; Arjuman, A.; Suneja, S.; Das, C.; Chandra, N. C. *Diabetes Vasc. Dis. Res.* **2012**, *9*, 196–204.
- (54) Johnson, G. D.; Stevenson, T.; Ahn, K. *J. Biol. Chem.* **1999**, *274*, 4053–4058.
- (55) Wang, S.; Wang, R.; Chen, L.; Bennett, D. A.; Dickson, D. W.; Wang, D.-S. *J. Neurochem.* **2010**, *115*, 47–57.
- (56) Padilla, B. E.; Cottrell, G. S.; Roosterman, D.; Pikiros, S.; Muller, L.; Steinhoff, M.; Bunnett, N. W. *J. Cell Biol.* **2007**, *179*, 981–997.
- (57) Lu, B.; Zhao, Y.; Zhao, J.; Yao, X.; Shuai, Y.; Ma, W.; Zhong, Y. *Protein Cell* **2016**, *7*, 606–610.
- (58) Chu, K. Y.; Briggs, M. J. L.; Albrecht, T.; Drain, P. F.; Johnson, J. D. *Islets* **2011**, *3*, 155–165.
- (59) Varlamov, O.; Fricker, L. D. *J. Cell Sci.* **1998**, *111*, 877–885.
- (60) Gavin, J. R.; Roth, J.; Neville, D. M.; De Meyts, P.; Buell, D. N. *Proc. Natl. Acad. Sci. U.S.A.* **1974**, *71*, 84–88.
- (61) White, M. F.; Kahn, C. R. *J. Biol. Chem.* **1994**, *269*, 1–4.
- (62) Morcavallo, A.; Stefanello, M.; Iozzo, R. V.; Belfiore, A.; Morrione, A. *Front. Endocrinol.* **2014**, *5*, 220.
- (63) Okuda, S.; Watanabe, Y.; Moriya, Y.; Kawano, S.; Yamamoto, T.; Matsumoto, M.; Takami, T.; Kobayashi, D.; Araki, N.; Yoshizawa, A. C.; Tabata, T.; Sugiyama, N.; Goto, S.; Ishihama, Y. *Nucleic Acids Res.* **2017**, *45*, D1107–D1111.